Navy Experimental Diving Unit
321 Bullfinch Road
Panama City, FL 32407-7015

NEDU TR 02-10
August 2002

DEVELOPMENT AND VALIDATION OF 1.3 ATA PO_2-in-He DECOMPRESSION TABLES FOR THE MK 16 MOD 1 UBA

Authors: WAYNE A. GERTH, Ph.D.
Associate Investigator

THOMAS M. JOHNSON
CDR, MC, USN
Principal Investigator

2. METHODS

2.1. DECOMPRESSION TABLE CALCULATION

While the LEM model can be used to directly compute schedules for repetitive dives, it is not readily used to produce repetitive dive tables in the convenient format that such tables for air and MK 16 MOD 0 N_2-O_2 diving currently have in the U.S. Navy Diving Manual. In order to produce such tables for MK 16 MOD 1 He-O_2 diving, a method was developed to map the probabilistic LEM model onto a deterministic overpressure model similar to that previously used[12] to produce the MK 16 MOD 1 N_2-O_2 tables. The method parameterizes the deterministic model to compute schedules at any pre-specified risk of DCS. The resultant model is then readily used to produce tables for repetitive diving in the desired U.S. Navy Diving Manual format.

2.2.1. LEM TO EL-RTA MAPPING

The method is based on the presumption that a sufficiently large and heterogeneous data set of completed dive profiles contains all information required to parameterize a deterministic overpressure model. While different models in this class may use different means to compute compartmental gas tensions, with different conceptualizations of blood-tissue gas exchange and the underlying compartments in which this exchange occurs, they share a common essential feature of the "Haldanian" method of computing decompression: Ascent decisions are based on the value of an overpressure with respect to a Maximum Permissible Tissue Tension (MPTT). The MPTT, also called an MVAL (M), for each of $i=1, 2, \ldots, n$ modeled compartments is generally a function of depth, D, and a vector, β_i, of Ω fundamental parameters[1]:

$$M_{i,D} = f(\beta_i, D);\ \beta_i = [\beta_{i,1}, \ldots, \beta_{i,\Omega}]. \quad (1)$$

Note that the β_i are rows of an $n \times \Omega$ matrix, β:

$$\beta = \begin{bmatrix} \beta_1 \\ \vdots \\ \beta_n \end{bmatrix} = \begin{bmatrix} \beta_{1,1} & \cdots & \beta_{1,\Omega} \\ \vdots & & \\ \beta_{n,1} & \cdots & \beta_{n,\Omega} \end{bmatrix}. \quad (2)$$

A Haldanian decompression is begun by ascending to the shallowest allowed stop depth, D_λ, at which no compartmental gas tension exceeds the corresponding M_{i,D_λ}. Ascent to the next stop is then allowed when compartmental gas tensions decay to the point where none exceed the corresponding MVAL for the next stop; i.e., when the overpressure with respect to MVAL in all compartments first satisfies $\left(p_i - M_{i,D_{\lambda-1}}\right) \leq 0$,

[1] Equivalently, ascent decisions may be based on the value of a prevailing compartmental tissue ratio, or TR_i, where $TR_i = M_{i,D}/D$.

where p_i is the gas tension in the i^{th} compartment, and $M_{i,D_{\lambda-1}}$ is the compartmental MVAL for the next stop at depth $D_{\lambda-1}$. Thus, ascent to the next stop is allowed when:

$$\max\left[\left(p_i - M_{i,D_{\lambda-1}}\right), i = 1,2,...,n\right] = 0. \tag{3}$$

The compartment in which this end-stop maximum occurs is called the "controlling tissue" for that stop. Upon completion of ascent to the next stop, λ is decremented and the process is repeated with ascent to successively shallower stops until the diver is surfaced at depth D_0.

The objective is to find the values of parameters in a given deterministic overpressure model that enable it to produce decompression schedules that are as close as possible to those prescribed by another model, all essential features of which are considered to be embodied in a "standard" data set of N dive profiles completed by the other model. Ideally, all end-stop gas tensions in these profiles will satisfy Eq. (3) in the desired deterministic model. However, this satisfaction cannot generally be made exact, because the safe ascent criteria in the original model, as well as the number of compartments and their associated gas exchange kinetics, will not generally be the same as those in the deterministic model. The closest possible overall approximation is obtained by adjusting the n x Ω elements of the β matrix in the deterministic model to minimize the sum of squares given by

$$ss = \sum_{\eta=1}^{N}\left\{\sum_{\delta=1}^{\Delta_\eta}\left\{\sum_{\lambda=\Lambda_{\eta,\delta}}^{1}\left(\max\left[\left(p_{i,\eta,\delta,\lambda} - M_{i,D_{\lambda-1}}\right), i = 1,2,...,n\right]\right)^2\right\}\right\}, \tag{4}$$

where the summation in the η^{th} profile is over all of the $\Lambda_{\eta,\Delta_\eta}$ decompression stops in each of the Δ_η dives in the profile, and $p_{i,\eta,\delta,\lambda}$ is the gas tension in the i^{th} compartment at the end of decompression stop λ in dive δ of the η^{th} profile as evaluated using the blood-tissue gas exchange kinetics of the deterministic model.

Depending on the structure of any given standard data set schedule, the pressure dependence of the MVALs, and the relation of surfacing MVALs to compartmental gas exchange kinetics, the argument of the square in Eq. (4) can be negative at any given stop. If this occurs at a sufficient number of stops throughout the standard data set schedules, ss minimization drives the M_i towards zero and the process fails. However, in what might be called "well-behaved" Haldanian models, the controlling tissue at any stop is also the tissue with the maximum prevailing gas tension at the end of the stop. Under such conditions, ascent occurs when the overpressure with respect to MVAL in the controlling tissue decays to zero, and Eq. (3) is replaced by:

$$\left(p_i - M_{i,D_{\lambda-1}}\right)\Big|_{p_{i,\max}} = 0, \tag{5}$$

where $P_{i,max}$ is the maximum compartmental gas tension at the end of stop λ. This behavior is forced in the *ss* minimization process by using the following in place of Eq. (4):

$$ss = \sum_{\eta=1}^{N}\left\{\sum_{\delta=1}^{\Delta_\eta}\left\{\sum_{\lambda=\Lambda_{\eta,\delta}}^{1}\left(\left(p_{i,\eta,\delta,\lambda} - M_{i,D_{\lambda-1}}\right)_{p_{i,\eta,\delta,\lambda,\max}}\right)^2\right\}\right\}, \qquad (6)$$

where the squared quantity is the overpressure with respect to MVAL in the controlling tissue at the end of decompression stop λ in dive δ of the η^{th} profile as evaluated using the blood-tissue gas exchange kinetics of the deterministic model. Use of Eq. (6) in place of Eq. (4) can avert failure of the *ss* minimization processes in these cases.

The $p_{i,\eta,\delta,\lambda}$ in either Eq. (4) or (6) also depend on additional parameters, such as the compartmental time constants for blood-tissue gas exchange, that in principle can also be adjusted in the *ss* minimization process. In present work, these parameters were considered to be intrinsic parts of the deterministic model definition, and were consequently fixed at pre-specified values. This left the β matrix as the only adjustable part of the deterministic algorithm, which reduced the overall number of adjustable parameters.

Minimization of either Eq. (4) or (6) requires a standard data set that is sufficiently large and heterogeneous to include profiles that exercise as much of the final MVAL domain as possible. Many of the profiles in the standard set may be well outside the range of profiles that one would advocate actually be dived.

The β extracted from the standard set by *ss* minimization is then used with the appropriate form of Eq. (1) to generate a table of MVALs that can in turn be used in the classical overpressure algorithm in real-time mode, or to generate decompression tables in U.S. Navy Diving Manual format. If the model approximated by the deterministic model is a probabilistic model, the resultant MVALs can be called PVALs to denote that the deterministic model embodies an essential feature of the probabilistic model; control of DCS risk according to an explicit acceptable risk scheme. An advantage of the approach in such cases is that decompression tables computed using the final deterministic model can be checked for conformance to the originally specified DCS risk scheme by evaluating the DCS risks of the schedules using the original probabilistic model. The entire process is schematized in Figure 3.

In the versions of the EL-RTA algorithm used to compute decompression tables for the MK 16 MOD 0 constant 0.7 ATA PO_2 UBA, a convention used by Workman[13] was adopted to make compartmental MPTT increase linearly with stop depth, *D*, giving Eq. (1) the following explicit form:

$$M_i = M_{0,i} + a_i D \; ; \; i=1, \ldots, n \, , \qquad (7)$$

where $M_{0,i}$ is the "surfacing" MPTT and a_i is a slope parameter. Referring to Eq. (1), the β_i vector under this convention is $\beta_i = [M_{0,i}, a_i]$, and an MPTT Table for n compartments with pre-specified blood-tissue gas exchange half-times is completely specified by nx2 parameters. This form for $f(\beta,D)$ was retained in present work, but it should be noted that the EL-RTA does not preclude use of more complex formulations.

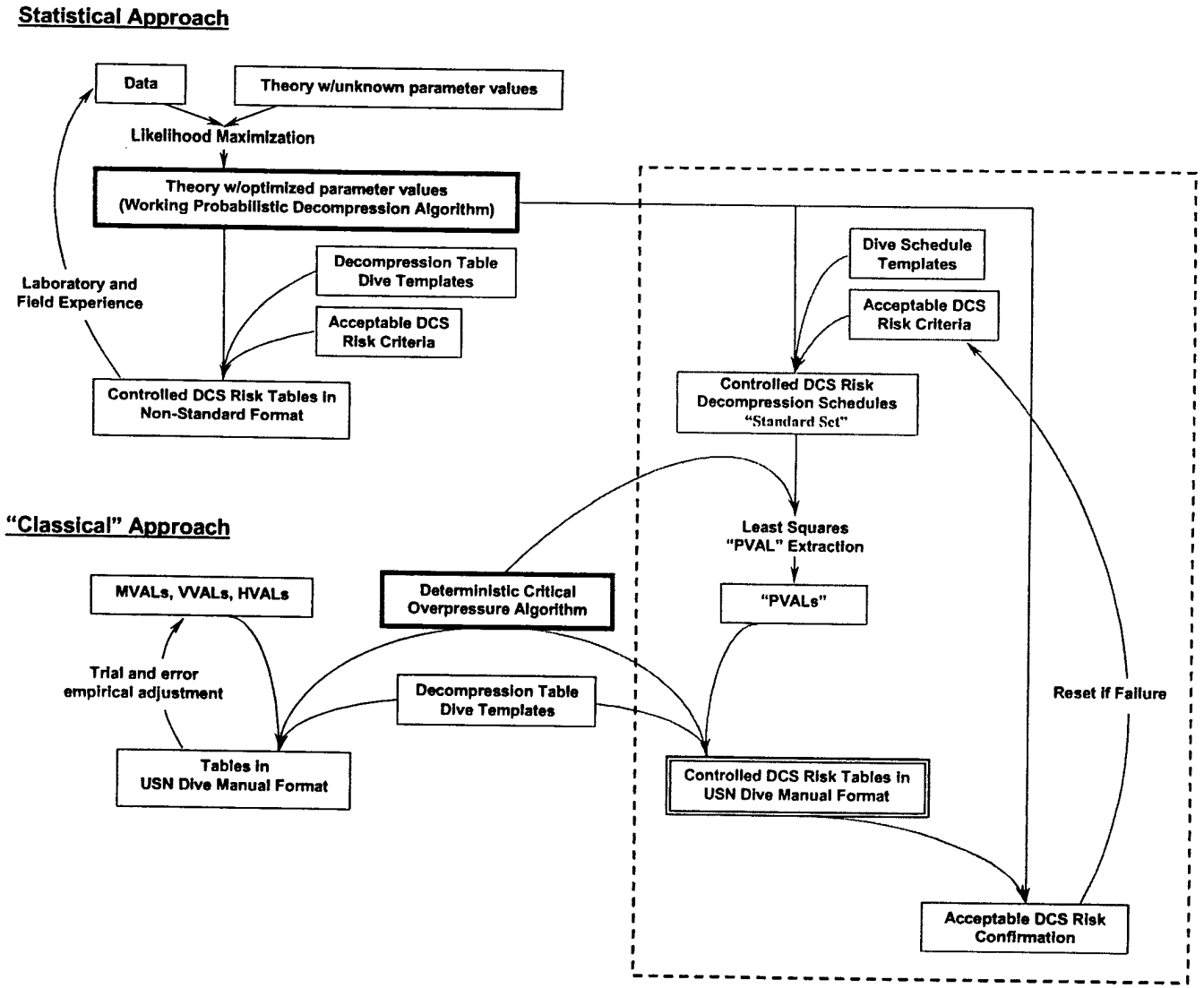

Figure 3. Table development schematic. Processes in the dotted line are used to parameterize a classical approximation of a statistical model and produce statistically based decompression tables in standard U.S. Navy Diving Manual format.

All parameters of the β matrix for the $f(\beta,D)$ function were successfully recovered except those for the 5-minute half-time compartment.

The complete process outlined in Figure 3 was then used with Eq. (4) to extract PVALs for the EL MK 15/16 RTA from profiles completed by the LEM model described in Section 1.2 and Appendix A. A standard set of 6,250 MK 16 MOD 1 He-O_2 dive profiles was built by first assembling profile templates in which the properties of each profile were specified by random selection from the pools of possible properties given in Table 8. These templates included breathing gas composition changes as per idealized MK 16 MOD 1 performance with 88/12 ($F_{I_{He}}/F_{I_{O_2}}$) as the diluent gas: The diver was assumed to breathe a 0.7 ATA PO_2-in-He mixture starting with descent from surface and continuing until arrival at 33 fsw, whereupon the inspired PO_2 was assumed to be 1.3 ATA-in-He for the remainder of the descent, time on the bottom, and subsequent ascent to 12 fsw. The inspired PO_2 was then assumed to be 0.7 ATA-in-He for the remaining ascent from 12 fsw to surface, after which the diver was assumed to breathe air. The LEM model was used to complete these templates at 2.3% fixed conditional DCS risk with 20 fsw as the shallowest allowed decompression stop.

The β matrix for a 9-compartment single-gas deterministic EL-RTA was then extracted from these profiles after setting each inspired inert gas fraction equal to the sum of the inspired N_2 and He fractions:

$$F_{I_{N_2}} = 1 - F_{I_{O_2}} = F_{I_{N_2}} + F_{I_{He}}. \qquad (8)$$

Results are given Table 10.

Table 10. Extracted β for Single-Gas EL RTA Approximation of LEM.

Compartmental Half-Time (min)	Extracted β	
	M_0 (atm)	Slope, a
5	3.8862658847	0.33419042769
10	3.2530411741	0.80040718224
20	1.6516881159	1.0244650367
40	2.1573713860	1.0501531224
80	1.9442800335	1.0875015513
120	0.88439535826	1.2477082949
160	0.71938369704	1.1325581371
200	1.0619074770	0.89880196526
240	0.77353416931	0.90032370927

Eq. (7) was then used with the extracted β in Table 10 to produce the table of Maximum Permissible Tissue Tensions (PVALs) given in Table 11 for final parameterization of the EL-RTA.

Table 11. PVAL Table for Single-Gas EL RTA Approximation of LEM.

TABLE OF MAXIMUM PERMISSIBLE TISSUE TENSIONS

(xval_he_4 - HELIUM)

TISSUE HALF-TIMES

DEPTH	5 MIN 1.00 SDR	10 MIN 1.00 SDR	20 MIN 1.00 SDR	40 MIN 1.00 SDR	80 MIN 1.00 SDR	120 MIN 1.00 SDR	160 MIN 1.00 SDR	200 MIN 1.00 SDR	240 MIN 1.00 SDR
10 FSW	131.892	115.608	64.879	81.863	75.188	41.731	35.121	44.114	34.590
20 FSW	135.234	123.613	75.124	92.365	86.063	54.208	46.447	53.102	43.594
30 FSW	138.576	131.617	85.369	102.866	96.938	66.685	57.773	62.090	52.597
40 FSW	141.918	139.621	95.613	113.368	107.813	79.162	69.098	71.078	61.600
50 FSW	145.260	147.625	105.858	123.869	118.688	91.640	80.424	80.066	70.603
60 FSW	148.602	155.629	116.103	134.371	129.563	104.117	91.749	89.054	79.606
70 FSW	151.944	163.633	126.347	144.872	140.438	116.594	103.075	98.042	88.610
80 FSW	155.286	171.637	136.592	155.374	151.313	129.071	114.401	107.030	97.613
90 FSW	158.627	179.641	146.837	165.876	162.188	141.548	125.726	116.018	106.616
100 FSW	161.969	187.645	157.081	176.377	173.063	154.025	137.052	125.006	115.619
110 FSW	165.311	195.649	167.326	186.879	183.938	166.502	148.377	133.994	124.623
120 FSW	168.653	203.653	177.570	197.380	194.813	178.979	159.703	142.982	133.626
130 FSW	171.995	211.657	187.815	207.882	205.688	191.456	171.028	151.970	142.629
140 FSW	175.337	219.661	198.060	218.383	216.563	203.933	182.354	160.958	151.632
150 FSW	178.679	227.666	208.304	228.885	227.438	216.410	193.680	169.946	160.636
160 FSW	182.021	235.670	218.549	239.386	238.313	228.887	205.005	178.934	169.639
170 FSW	185.363	243.674	228.794	249.888	249.188	241.365	216.331	187.922	178.642
180 FSW	188.705	251.678	239.038	260.389	260.063	253.842	227.656	196.910	187.645
190 FSW	192.046	259.682	249.283	270.891	270.938	266.319	238.982	205.898	196.649
200 FSW	195.388	267.686	259.528	281.392	281.813	278.796	250.307	214.886	205.652
210 FSW	198.730	275.690	269.772	291.894	292.688	291.273	261.633	223.874	214.655
220 FSW	202.072	283.694	280.017	302.395	303.563	303.750	272.959	232.862	223.658
230 FSW	205.414	291.698	290.262	312.897	314.438	316.227	284.284	241.850	232.661
240 FSW	208.756	299.702	300.506	323.398	325.313	328.704	295.610	250.838	241.665
250 FSW	212.098	307.706	310.751	333.900	336.188	341.181	306.935	259.826	250.668
260 FSW	215.440	315.710	320.996	344.401	347.063	353.658	318.261	268.814	259.671
270 FSW	218.782	323.714	331.240	354.903	357.938	366.135	329.587	277.802	268.674
280 FSW	222.124	331.718	341.485	365.405	368.813	378.612	340.912	286.790	277.678
290 FSW	225.465	339.722	351.730	375.906	379.688	391.089	352.238	295.778	286.681
300 FSW	228.807	347.726	361.974	386.408	390.563	403.567	363.563	304.766	295.684

BLOOD PARAMETERS

(PRESSURE IN FSW; 33 FSW/ATA)

PACO2	PH2O	PVCO2	PVO2	AMBAO2	PBOVP
1.50	0.00	2.30	2.00	0.00	0.000

The pressure dependence of the PVALs in Table 11 is illustrated in Figure 12. In accord with the form for the *f(β,D)* function adopted in present work, PVALs exhibit the linearity typical of the VVALs and HVALs of Thalmann's earlier versions of the EL-RTA. However, the present PVALS for different half-time compartments increase with depth along different slopes, which departs from the parallelism of the lines for the different compartments in similar plots of the earlier MPTTs.

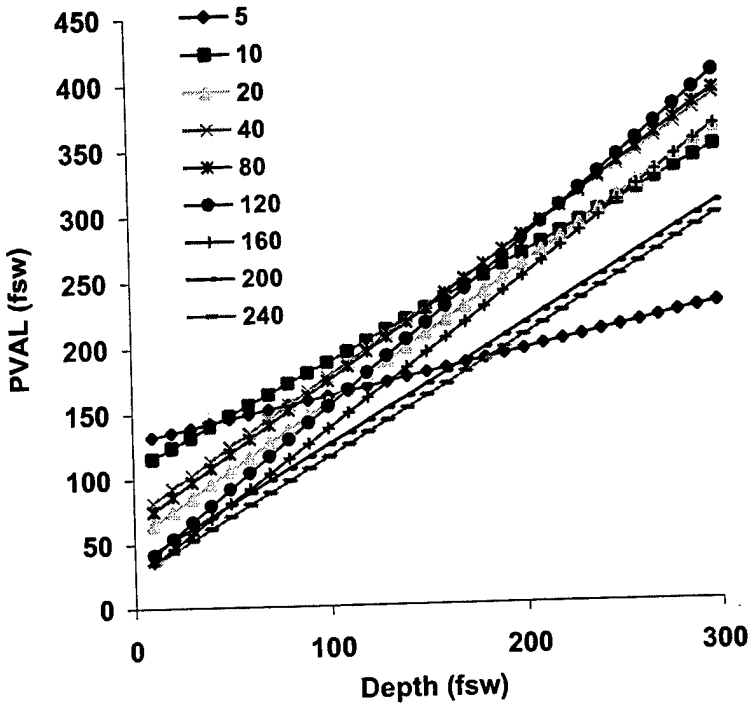

Figure 12. Depth-dependence of compartmental PVALs in the EL RTA approximation of LEM.

The EL-RTA with the XVAL-He-4 MPTT table was used to produce the parts of new MK 16 MOD 1 HeO_2 decompression tables in which repetitive diving is supported; *i.e.*, schedules for dives to depths of 200 fsw or less. The 120-minute half-time

computed using the EL-RTA in its "real-time" mode, where the schedule for each repetitive dive is based on the model state at the end of the preceding surface interval. Such schedules tend to be less conservative than those prescribed by the tables *per se* because in the latter

- washout of residual gas during surface intervals is presumed to be governed by a single, relatively slow 120-min half-time reference compartment;
- washout of residual gas from the reference compartment during surface intervals is presumed to start from the maximum gas tension allowed in the surfacing repetitive group, and;
- adjusted bottom times are rounded-up to the next largest tabulated bottom time.

A comparison of each repetitive dive schedule selected for test to its corresponding schedule as prescribed by the MK 16 MOD 1 He-O_2 decompression Tables is given in Appendix K.

3.4. PHASE II DIVE TRIAL

A total of 299 man-exposures were completed on 37 different dive profiles in Phase II of the program. A description of the profiles, with the number of exposures and DCS outcome for each profile, is given in Appendix D.

3.4.1. DCS INCIDENCE AND OTHER OUTCOMES

Six DCS cases occurred in the 299 exposures in this program phase, yielding an overall observed DCS incidence of 2.01%. Again, as in the description of the Phase I results, it can be asserted at 95% confidence that the overall DCS risk of the profiles is less than 4.32% under the null hypothesis that the observed DCS incidence was in fact the true DCS risk of the 299 exposures.

Other medical events in this program phase are described in Appendix F.

APPENDIX A.

DCS Model Descriptions

The different decompression algorithms used in the present work provide a means to compute gas contents of diver tissues throughout a dive profile so that the profile can be configured to keep those contents always within limits associated with acceptable incidences of DCS.

The algorithms are based on the conceptualization shown in Figure A1, when the diver is presumed to be breathing a mixture of oxygen in m inert gases. Parts of the body involved in the etiology of DCS are considered to consist of a series of n parallel-perfused, well-stirred gas exchange compartments, or "tissues," as shown in panel A. A detail of one compartment is shown in panel B. Subscript g for arterial, venous, and tissue gas tensions ranges from 1 to $m+j$, where j=1 if oxygen is considered to contribute dynamically to each compartmental sum of dissolved gas tensions in a multiple gas model, or j=0 otherwise. p_{fix} denotes the sum of the tensions of water vapor, carbon dioxide, and oxygen that are assumed constant and uniform throughout the modeled compartments [see Eq. (A4) below]. Gas exchange between tissue and blood in each compartment is assumed to be perfusion limited, so that the tension of a gas g in venous blood leaving the tissue equals the tension of that gas in the tissue: $p_{v,i,g} = p_{t,i,g}$.

In a subject breathing air or N_2O_2, arterial blood is assumed to be always equilibrated with alveolar gas having an N_2 partial pressure $P_{A_{N_2}}$ at ambient barometric pressure P_{amb} given by rearrangement of the alveolar gas equation[1] for no CO_2 in the inspired gas ($P_{I_{CO_2}} = 0$):

$$p_{a,N_2} = P_{A_{N_2}} = F_{I_{N_2}} \cdot \{(P_{amb} - P_{H_2O}) - P_{A_{CO_2}} (1 - 1/RQ)\}, \qquad \text{(A1)}$$

where p_{a,N_2} is the arterial inert gas tension, $F_{I_{N_2}} = 1 - F_{I_{O_2}}$ is the N_2 fraction in dry inspired gas, RQ is the respiratory quotient, and $P_{A_{CO_2}}$ is the alveolar carbon dioxide partial pressure. The latter, along with water vapor pressure, P_{H_2O}, is assumed to remain constant. Equation (A1) is generalized for each of m inspired inert gases:

$$p_{a,g} = F_{I_g} \cdot \left\{(P_{amb} - P_{H_2O}) - P_{A_{CO_2}} (1 - 1/RQ)\right\}; g = 1, \ldots, m \qquad \text{(A2)}$$

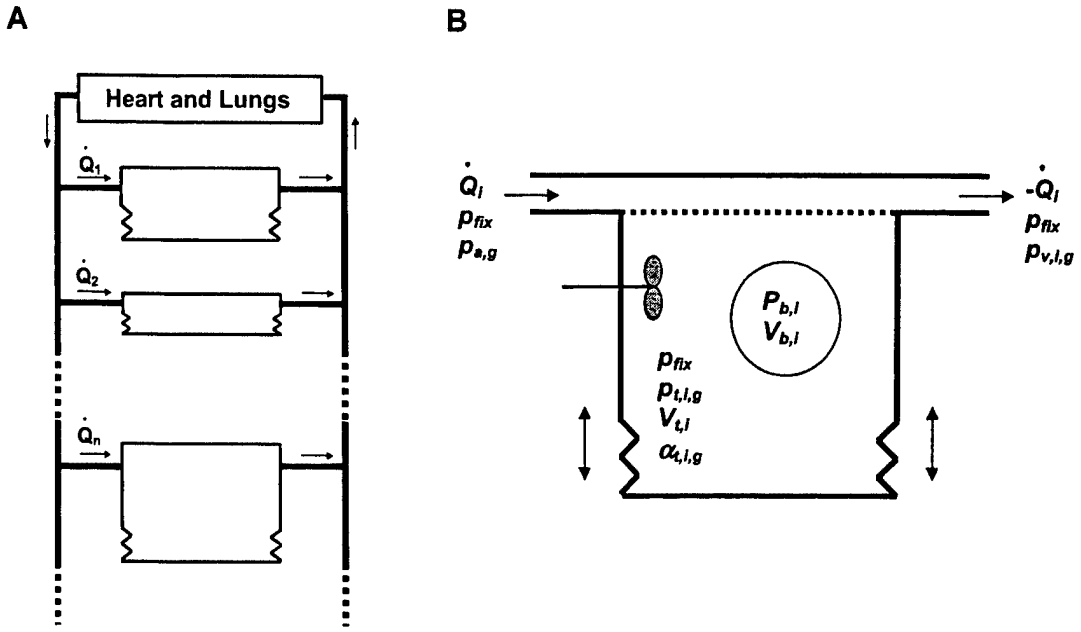

Figure A1. Schematic of the LEM model, in which the subject is assumed to be breathing a mixture of oxygen in m inert gases. A) n parallel-perfused compartment model of whole body. Association of compartments with specific anatomical sites is disclaimed, except to assert that the modeled compartments represent tissues or tissue components that are involved in the occurrence of DCS. B) Detail of compartment in (A). The jagged lines with double-headed arrows indicate that the overall volume of the compartment, $(V_{t,i}+V_{b,i})$, varies with bubble volume, while the compartmental liquid volume, $V_{t,i}$, remains constant.

The dissolved gas tension of gas g in the i^{th} compartment, $p_{t,i,g}$, at any time t in a profile stage is given generally by the expression for mass balance between bubble, tissue, and blood in a perfusion-limited system:

$$\frac{dp_{t,i,g}}{dt} = \frac{k_g \cdot t + (p^o_{a,g} - p_{t,i,g})}{\tau_{i,g}} - \left(\frac{1}{\alpha_{t,i,g} V_t}\right)\left(\frac{d\left(P_{b,i,g} V_{b,i}\right)}{dt}\right) - Z_{met,i,g} \quad ; g=1, \ldots, m+j, \qquad \text{(A3)}$$

where $RT(P_{b,i,g}V_{b,i})$ is the number of moles of gas g at partial pressure $P_{b,i,g}$ in a bubble of volume $V_{b,i}$; $p^o_{a,g}$ is the arterial tension of the gas at t^o, the beginning of the stage; and $Z_{met,i,g}$ is the rate at which the gas is consumed by metabolic processes in the tissue. With $p_{a,g}$ equal to the arterial tension of the gas at time t, k_g is the rate of change of the arterial gas tension during the stage:

$$k_g = \frac{p_{a,g} - p^o_{a,g}}{t - t^o}. \qquad \text{(A3.a)}$$

The compartmental time constant, $\tau_{i,g}$, is given in terms of the Ostwald solubility of the gas in the compartment, $\alpha_{t,i,g}$; the compartmental volume, $V_{t,i}$; the compartmental blood flow, $\dot{Q}_i$; and the Ostwald solubility of the gas in blood, $\alpha_{blood,g}$:

$$\tau_{i,g} = \frac{\alpha_{t,i,g} V_{t,i}}{\alpha_{blood,g} \dot{Q}_i} . \qquad \text{(A3.b)}$$

The compartmental half-time, $t_{1/2,i,g}$, or the time required to halve an initial tissue-blood gas tension difference with constant $\tau_{i,g}$ and $p_{a,g}$, is then given by

$$t_{1/2,i,g} = \ln(2) \cdot \tau_{i,g} \cong 0.693 \cdot \tau_{i,g} \qquad \text{(A3.c)}$$

Note that $\dot{Q}_i$ in Eq. (A3.b) is the blood flow to the entire compartmental volume per unit time, not the perfusion rate obtained by normalizing this flow to the compartmental volume.

Unless otherwise noted, Z_{met,i,O_2} for oxygen is assumed always to have values sufficient to keep the tissue p_{O_2} constant and the same in all compartments. The index j in the above equations is then 0, and the tissue p_{O_2} is added to the other fixed gas tensions, p_{CO_2} and P_{H_2O}, to define a compartment-independent constant:

$$p_{fix} = P_{H_2O} + p_{CO_2} + p_{O_2} . \qquad \text{(A4)}$$

On the other hand, if Z_{met,i,O_2} is too small to keep the tissue p_{O_2} constant, oxygen may contribute dynamically to the overall compartmental dissolved gas content. In order to simulate and track these contributions, oxygen in excess of a certain arterial tension $PSET_i$ is considered to behave as an inert gas that follows Henry's law in blood and tissue. Under these conditions j=1, and quantities with subscript g=m+1 in the above equations correspond to compartmental O_2 contents that arise from this excess arterial O_2, where

$$p_{a,O_2} = 0 \qquad \text{if } P_{A_{O_2}} \le PSET_i , \qquad \text{(A5)}$$

$$p_{a,O_2} = P_{A_{O_2}} - PSET_i \qquad \text{if } P_{A_{O_2}} > PSET_i , \qquad \text{(A6)}$$

and [see Eq. (A2)]

$$P_{A_{O_2}} = P_{amb} - P_{H_2O} - P_{A_{CO_2}} - \sum_{g=1}^{m} p_{a,g} . \qquad \text{(A7)}$$

Note that specification of a sufficiently high value of $PSET_i$ forces a constant compartmental p_{O_2}, which is equivalent to setting j=0 for the compartment.

For each of the $m+j$ "inert" gases that by definition are not reactants or products of tissue metabolism, the $Z_{met,i,g}$ term vanishes and Eq. (A3) simplifies to

$$\frac{dp_{t,i,g}}{dt} = \frac{k_g \cdot t + (p^o_{a,g} - p_{t,i,g})}{\tau_{i,g}} - \left(\frac{1}{\alpha_{t,i,g} V_t}\right)\left(\frac{d(P_{b,i,g} V_{b,i})}{dt}\right) ; g=1, \ldots, m+j. \qquad \text{(A8)}$$

In the absence of a bubble, the rightmost term in Eq. (A8) vanishes so that each gas exchanges between tissue and blood independently. The analytic solution of the resultant expression is used to determine the tension of gas g in tissue at any time t:

$$p_{t,i,g} = p^o_{a,g} + \left(p^o_{t,i,g} - p^o_{a,g}\right) \cdot \exp\left(\frac{-t}{\tau_{i,g}}\right) + k_g t + k_g \tau_{i,g}\left\{\exp\left(\frac{-t}{\tau_{i,g}}\right) - 1\right\}, \qquad \text{(A9)}$$

where $p^o_{t,i,g}$ is the compartmental inert gas tension at t=0.

Impact of Bubble Evolution

Once a bubble has nucleated in a compartment at time t_{bf} in a profile stage, its subsequent evolution affects blood-tissue gas exchange kinetics and renders Eq. (A9) inapplicable. Blood-tissue gas exchange kinetics are then considered in terms of the compartmental inert gas burden $P'_{t,i}$, defined as the sum of the dissolved inert gas tension and the inert gas tension that would be exerted by the undissolved inert gas in bubbles if that gas had remained in solution. The differential equation for $P'_{t,i}$ is obtained by rearranging Eq. (A8) for each gas and collecting terms:

$$\frac{dP'_{t,i}}{dt} = \sum_{g=1}^{m+j}\left\{\frac{dp_{t,i,g}}{dt} + \left(\frac{1}{\alpha_{t,i,g} V_{t,i}}\right)\left(\frac{d(P_{b,i,g} V_{b,i})}{dt}\right)\right\} = \sum_{g=1}^{m+j}\left\{\frac{\left[k_g t - \left(p_{t,i,g} - p^o_{a,g}\right)\right]}{\tau_{i,g}}\right\}. \qquad \text{(A10)}$$

Note that in the absence of bubbles, $P'_{t,i} = \sum_{g=1}^{m+j} p_{t,i,g}$, where the $p_{t,i,g}$ are given by Eq. (A8).

The bubble is assumed to be always in equilibrium with its surroundings, so that $p_{t,i,g} = P_{b,i,g}$ for g=1, ..., $m+j$ and $p_{fix} = P_{fix}$, where p_{fix} is given by Eq. (A4) and P_{fix} is the sum of the fixed gas partial pressures in the bubble. The sum of the inert gas partial pressures in the bubble is then given by the Laplace equation, which with neglect of mechanical effects from tissue deformation is

$$\sum_{g=1}^{m+j} P_{b,i,g} = P_{amb} - P_{fix} + \frac{2\sigma}{r_i} , \qquad \text{(A11)}$$

where σ is the gas-liquid surface tension and r_i is radius of the bubble. This equation indicates that the total gas pressure in the bubble exceeds the ambient pressure by an amount equal to the surface pressure, $2\sigma/r_i$. Neglecting the dependence of the surface pressure on r_i, the contribution of the surface pressure to the bubble pressure is simplified by setting the surface pressure equal to a constant of value PXO_i, so that Eq. (A11) is written

$$\sum_{g=1}^{m+j} P_{b,i,g} = P_{amb} - P_{fix} + PXO_i . \qquad \text{(A12)}$$

It follows from the assumed equilibrium between bubble and tissue that the sum of the tissue tensions equals the sum of the bubble partial pressures, so that we have from Eq. (A12) that

$$\sum_{g=1}^{m+j} p_{t,i,g} = \sum_{g=1}^{m+j} P_{b,i,g} = P_{amb} - P_{fix} + PXO_i , \qquad \text{(A13)}$$

which couples the sum of the tissue tensions to the ambient hydrostatic pressure.

Single inert gas dynamics: The Exponential-Linear Real-Time Algorithm (EL-RTA)

When a subject breathes a mix that contains only a single inert gas, m=1 and j=0, and Eq. (A13) reduces to

$$p_{t,i} = P_{b,i} = P_{amb} - P_{fix} + PXO_i , \qquad \text{(A14)}$$

where we suppress expression of the subscript g because it is always 1. The dissolved inert gas tension in tissue is given directly in terms of the ambient hydrostatic pressure, and the simple expressions for the exponential-linear (EL) model are obtained. Thus, if ambient pressure changes are also always considered time-linear, Equation (A14) becomes

$$p_{t,i} = P_{b,i} = k_p(t - t_{bf}) + P_{bf} - P_{fix} + PXO_i , \qquad \text{(A15)}$$

where k_p is the rate of change of the hydrostatic pressure during the stage and P_{bf} is the hydrostatic pressure at t=t_{bf}. If the stage was entered with a bubble already present, t_{bf}=0 and $P_{bf} = P^o_{amb}$. Substitution into Equation (A10) then yields

$$\frac{dP'_{t,i}}{dt} = TC_i \cdot \left[p_a^o + (k - k_p)(t - t_{bf}) - P_{bf} + P_{fix} - PXO_i\right], \qquad \text{(A16)}$$

where $TC_i = 1/\tau_i$, p_a^o is evaluated at $t=t_{bf}$, and k is given for the single inert gas by Eq. (A3.a). Integration of this expression from t_{bf} to t yields the EL model expression for the compartmental inert gas burden at any time t in a profile stage when a bubble is present:

$$P'_{t,i} = P'^{o}_{t,i} + TC_i \cdot \left\{\left(p_a^o - p_{bf} + P_{fix} - PXO_i\right)\cdot(t - t_{bf}) + \left[(k - k_p)/2\right]\cdot(t - t_{bf})^2\right\}, \qquad \text{(A17)}$$

where $P'^{o}_{t,i}$ is the inert gas burden at $t=t_{bf}$. Eq. (A17) is readily cast in the form given by Parker, *et al.*[2] by recalling that $p_a^o = P_{amb}^o - p_{a_{O_2}}^o - p_{a_{CO_2}}^o - P_{H_2O}$ and that arterial blood is assumed to be in equilibrium with alveolar gas:

$$P'_{t,i} = P'^{o}_{t,i} + TC_i \cdot \left\{\left(p_{t_{O_2}} + p_{t_{CO_2}} - P^o_{A_{O_2}} - P^o_{A_{CO_2}} - PXO_i\right)\cdot(t - t_{bf}) - \left[k_{O_2}/2\right]\cdot(t - t_{bf})^2\right\}, \quad \text{(A17.a)}$$

where $k_{O_2} = k_p - k$ is the rate of change of the alveolar oxygen pressure in the stage.

Under the assumed equilibrium of the bubble with its surroundings, Eq. (A8) is solved to obtain the following expression for the rate of change of bubble volume at constant ambient pressure and p_a:[3]

$$\frac{dV_{b,i}}{dt} = \alpha_{blood}\dot{Q}_i\left(\frac{p_a}{p_{t,i}} - 1\right). \qquad \text{(A18)}$$

Eq. (A15) is readily shown to imply that the bubble volume must decrease monotonically during any isobaric stage in which p_a is constant after decompression. Eq. (A15) is also readily integrated to obtain an analytical solution for $V_{b,i}$, which contrasts with the required resort to numerical methods in the Linear-Exponential Multiple Gas, or LEM model below.

Multiple inert gas dynamics: The Linear-Exponential Multiple Gas Model (LEM)

When a gas mix with more than one inert gas is breathed, Eq. (A10) must be solved numerically. The individual $p_{t,i,g}$ are obtained by rearranging the expression for the total number of moles of each gas in the tissue;

$$n_{i,g} = \alpha_{t,i,g}p_{t,i,g} + \frac{p_{t,i,g}V_{b,i}}{RT}; \qquad \text{(A19)}$$

to yield:

$$p_{t,i,g} = \frac{n_{i,g}}{\alpha_{t,i,g} + V_{b,i}/RT}. \tag{A20}$$

The first term on the right of Eq. (A19) is the amount of gas g in solution, and the second term is the amount of undissolved gas g in one or more bubbles. If we let $X_i = V_{b,i}/RT$ and note that the contribution of gas g to the overall inert gas burden is simply $P'_{t,i,g} = \frac{n_{i,g}}{\alpha_{t,i,g}}$, Eq. (A20) becomes

$$p_{t,i,g} = \frac{P'_{t,i,g}}{1 + X_i/\alpha_{t,i,g}}. \tag{A21}$$

At any time, all compartmental quantities except X_i are known for determination of the individual $p_{t,i,g}$. The unknown X_i is obtained by substituting Eq. (A20) into Eq. (A13). Rearrangement then yields a homogeneous polynomial of the order $m+j$ with positive real root equal to X_i. This root is determined by standard methods and updated for each time step in the numerical solution of Eq. (A10) as $n_{i,g}$ and $p_{t,i,g}$ change with time.

For example, when $m+j=2$, Eq. (A13) becomes

$$\sum_{g}^{m+j} p_{t,i,g} = \frac{n_{i,1}}{\alpha_{t,i,1} + V_{b,i}/RT} + \frac{n_{i,2}}{\alpha_{t,i,2} + V_{b,i}/RT} = P_{amb} - P_{fix} + PXO_i, \tag{A22}$$

which rearranges to

$$0 = A_i X_i^2 + B_i X_i + C_i \tag{A23}$$

where

$$A_i = P_{amb} - P_{fix} + PXO_i, \tag{A23.a}$$

$$B_i = \left\{A_i\left(\alpha_{t,i,2} + \alpha_{t,i,1}\right) - \left(n_{i,1} + n_{i,2}\right)\right\}, \tag{A23.b}$$

$$C_i = \left\{A_i \alpha_{t,i,1}\alpha_{t,i,2} - \left(n_{i,1}\alpha_{t,i,2} + n_{i,2}\alpha_{t,i,1}\right)\right\}. \tag{A23.c}$$

The quadratic Equation (A23) has positive real root given by

$$X_i = \frac{-B_i + \sqrt{B_i^2 - 4A_iC_i}}{2A_i}. \tag{A24}$$

Similarly, when $m+j=3$, Eq. (A13) becomes

$$0 = A_i X_i^3 + B_i X_i^2 + C_i X_i + D_i \qquad \text{(A25)}$$

where A_i is as defined in Eq. (A23.a) and

$$B_i = \left\{A_i\left(\alpha_{t,i,1} + \alpha_{t,i,2} + \alpha_{t,i,3}\right) - \left(n_{i,1} + n_{i,2} + n_{i,3}\right)\right\} \qquad \text{(A25.a)}$$

$$C_i = A_i\left(\alpha_{t,i,1}\alpha_{t,i,2} + \alpha_{t,i,1}\alpha_{t,i,3} + \alpha_{t,i,2}\alpha_{t,i,3}\right) - \left[n_{i,1}\left(\alpha_{t,i,2} + \alpha_{t,i,3}\right) + n_{i,2}\left(\alpha_{t,i,1} + \alpha_{t,i,3}\right) + n_{i,3}\left(\alpha_{t,i,1} + \alpha_{t,i,2}\right)\right] \qquad \text{(A25.b)}$$

$$D_i = A_i\alpha_{t,i,1}\alpha_{t,i,2}\alpha_{t,i,3} - \left(n_{i,1}\alpha_{t,i,2}\alpha_{t,i,3} + n_{i,2}\alpha_{t,i,1}\alpha_{t,i,3} + n_{i,3}\alpha_{t,i,1}\alpha_{t,i,2}\right). \qquad \text{(A25.c)}$$

The root X_i of Eq. (A25) is determined from Cardan's formula for cubic polynomials.[4]

Deterministic Models

Use of computed compartmental gas contents to schedule decompressions in deterministic or classical overpressure models is discussed in Section 2.2.1. Present work was commenced using software described by Thalmann, which implements the Haldanian method of computing decompression using the single-gas LE model of whole-body gas uptake and elimination.[5,6,7] This software was enhanced to support the added requirements of present work.

Probabilistic Models and DCS risk

Probabilistic models require an additional function to relate the inert gas burden to the probability of DCS occurrence. For these purposes, DCS, irrespective of its particular manifestation or severity, is assumed only to occur or not occur in any dive profile. The probability, $P_{DCS}(t)$, that an individual will suffer DCS by any time t in a profile started at $t=0$ is then given in terms of the DCS risk function, $h(t)$:

$$P_{DCS}(t) = 1.0 - S(t) = 1.0 - \exp\left\{-\int_0^t h(t)dt\right\}, \qquad \text{(A26)}$$

where the survivor function, $S(t)$, is the probability that the individual will remain free of DCS up to time t.[8,9] The latter is defined as the joint probability of remaining DCS-free in each of the n compartments of the model schematized in Figure A1. Statistical independence of the compartmental outcomes is then assumed to define the risk function in terms of the time courses of the ambient pressure and inspired gas composition and their influences on compartmental dissolved gas contents and bubble volumes.

The instantaneous risk, $h(t)$, is defined as the weighted sum of the prevailing compartmental gas supersaturations, $SS_i(t)$, in excess of compartmental threshold values, Thr_i, relative to the ambient hydrostatic pressure, P_{amb}:[2]

$$h(t)=\sum_{i=1}^{n} G_i\left(SS_i(t)-Thr_i\right)/P_{amb}\ ;\quad SS_i(t)-Thr_i>0\,,$$

$$h(t)=0\ ;\qquad\qquad SS_i(t)-Thr_i\le 0\,, \tag{A27}$$

where G_i is a constant compartmental gain, and $SS_i(t)$ is given in terms of the prevailing compartmental inert gas burden:

$$SS_i(t)=P'_{t,i}-\left(P_{amb}-P_{fix}\right)\,. \tag{A27.a}$$

Implementation

In order to compute $h(t)$ throughout an arbitrarily complex profile of pressure and respired gas, the profile is encoded as a sequence of nodes each characterized by a pressure or depth, an inspired O_2 fraction, and a time elapsed since the preceding node. An unbroken description of the exposure profile is then obtained by linear interpolation in the time domain between pressures and respired O_2 fractions at successive nodes. Each node consequently describes the conditions prevailing at the end of a profile stage that is either a travel (compression or decompression) stage, an isobaric stage, a breathing gas switch stage, or a combination travel and breathing gas switch stage. The model is exercised on the profile by sequentially processing these stages, preserving the model state at the end of each stage as the initial state for the next.

Compartmental contributions to the cumulative DCS risk in Eq. (A26) were determined numerically by trapezoidal integration. DCS risk accumulation does not require the presence of a bubble, but occurs in any compartment whenever the hydrostatic pressure is less than a risk accumulation threshold pressure given by $\left(P'_{t,i}+P_{fix}-Thr_i\right)$. However, bubble formation and resolution still must be tracked in order to properly transition between the exponential kinetics of Eq. (A9) and the more complex kinetics that prevail after bubble formation (linear/quadratic kinetics, Eq. (A17), if $m+j=1$; nonlinear kinetics if $m+j>1$). Model equations for a compartment are consequently solved over small time steps as long as risk continues to accumulate or a bubble is present in the compartment. During most other periods, compartmental dissolved inert gas tensions are tracked analytically from node to node using Eq. (A9).

If a bubble is not present or DCS risk is not already accumulating in a compartment on advance to a new stage, the compartmental dissolved gas tensions at the stage start node and at the stage end node as evaluated with Eq. (A9) are examined to determine

whether a bubble will nucleate or DCS risk will begin to accumulate in the stage. Risk accumulation, bubble nucleation, or both will occur if the hydrostatic pressure is less than the risk accumulation threshold pressure or the EL bubble formation pressure, $\left(\sum_{g=1}^{m+j} p_{t,i,g} + P_{fix} - PXO_i \right)$, at either of the nodes.

At the start of a stage in which bubble nucleation or DCS risk accumulation occurs, processing is undertaken over dt_{min} time steps, switching from use of Eq. (A9) to Eq. (A17) or numerical solution of Eq. (A10), as appropriate. The integral compartmental contribution to the cumulative DCS risk is updated for each time step that starts or ends with a hydrostatic pressure less than the concurrent risk accumulation threshold pressure.

REFERENCES

1 West, J. B., *Respiratory Physiology*, 3rd ed. (Baltimore, MD: Williams and Wilkins, 1985).

2 Parker, E.C., Survanshi, S.S., Weathersby, P.K. and Thalmann, E.D. *Statistically Based Decompression Tables VIII: Linear-Exponential Kinetics*. NMRI Technical Report 92-73, Bethesda, MD: Naval Medical Research Institute, 1992.

3 Vann, R.D. (1982) Decompression Theory and Applications. In: Bennett, P.B. and Elliott, D.H., (Eds.) *The Physiology and Medicine of Diving and Compressed Air Work*, Third edn. (London: Bailliere Tindall, 1989) pp. 352-382.

4 Marcus, M. and Minch, H., *Modern University Algebra* (New York: MacMillan Company, 1966), pp. 200–201.

5 Thalmann, E. D. *Computer Algorithms Used in Computing the MK 15/16 Constant 0.7 ATA, Oxygen Partial Pressure Decompression Tables*. NEDU Report No. 1-83, Navy Experimental Diving Unit, Panama City, FL, 1983.

6 Thalmann, E. D. *Repetitive/Multi-Level Dive Procedures and Tables for Constant 0.7 ATA Oxygen Partial Pressure in Nitrogen Diving*. NEDU Report 9-85, Navy Experimental Diving Unit, Panama City, FL, 1985

7 Thalmann, E. D. NEDU Technical Memorandum TM 85-12, Enclosure (1), Navy Experimental Diving Unit, Panama City, FL, 1985.

8 Weathersby, P.K., Homer, L.D. and Flynn, E.T. (1984) On the likelihood of decompression sickness. *Journal of Applied Physiology: Respiration, Environmental and Exercise Physiology* **57** (3):815-825.

9 Gerth, W. A. Overview of Survival Analysis and Maximum Likelihood Techniques. Weathersby, P.K. and Gerth, W.A., (Eds.) *Workshop on Survival Analysis and Maximum Likelihood Techniques as Applied to Physiological Modeling*. Bethesda, MD: Undersea and Hyperbaric Medical Society. (*in press*)